

Numerical simulation of the draft tube and tailwater flow interaction

Simulation numérique de l'interaction entre le diffuseur et l'écoulement aval

WEIXING YUAN, *Research Assistant, Institute and Laboratory for Hydraulic Machinery and Plants, University of Technology Munich, 85747 Garching, Germany; presently visiting fellow at the Institute for Aerospace Research, National Research Council of Canada*

RUDOLF SCHILLING, *Professor Dr.-Ing. Dr.-Ing. habil., Head of the Institute and Laboratory for Hydraulic Machinery and Plants, University of Technology Munich, Germany*

ABSTRACT

This work focuses on the numerical simulation of the interaction between the draft tube and tailwater flow in low head hydro power plants. An approach to the solution of incompressible free surface flow problems is developed. The flow field and the free surface location are calculated by coupling the free surface kinematic and dynamic conditions with the equations of motion for the bulk flow. A pressure correction method is applied to the flow calculation in a moving grid system. The RNG k - ϵ model is used for turbulence modelling. In order to reduce the computational time, the PVM (Parallel Virtual Machine) subroutines are implemented.

RÉSUMÉ

Ce travail est centré sur la simulation numérique des écoulements et de l'interaction entre le diffuseur et l'aval dans les centrales hydro-électriques de basse chute. Une approche de la solution des problèmes d'écoulements à surface libre est développée. Le champ de vitesse et la position de la surface libre sont calculés en couplant les conditions cinématique et dynamique de surface libre avec les équations du mouvement moyen. On applique une méthode de correction de pression au calcul des vitesses dans un système de grille mouvante. La turbulence est prise en compte par le modèle k - ϵ RNG. Pour réduire le temps de calcul, le parallélisme est mis en œuvre avec des routines PVM.

1 Introduction

The theoretical and experimental investigations of Schneider et al. [14], [15] as well as Toyokura et al. [17] have shown that there is an interaction between the draft tube and tailwater flow. The work of Kita et al. [9] has also confirmed that the combination of the draft tube of water turbines with the open channel affects the efficiency and output of water power plants. It becomes a particularly more important problem for low head water turbines. This problem is being solved by a numerical simulation technique. This paper introduces a numerical scheme to compute viscous incompressible flows with free surface in a time-accuracy manner.

The numerical calculation of free surface problems in hydraulics and other fields is difficult considering non-rectangular and unknown geometry. The free surface must be adjusted iteratively until the surface conditions are satisfied. Many methods are available and have been used. To represent and follow the free surface the VOF (Volume of Fluid) method introduced by Hirt and Nichols [8] can be used whenever the grid is stationary. However, it is difficult both to apply the free surface boundary conditions and track the free surface in time, since the grid lines do not represent the free surface and the free surface develops itself in many grid lines. Another alternative, which uses a water level height function, is adopted in this work because of its accuracy in representing the free surface. The free surface elevation is determined using the free surface velocity in a moving grid system.

The fundamental problem in the prediction of incompressible flows, even flows without the complication of a free surface, is

the determination of the static pressure. Because the density is constant, a time-independent constraint must be imposed to couple changes of the velocity field with the pressure field while satisfying the continuity equation. One possibility is the artificial compressibility method proposed by Chorin [3]. The basic idea is to introduce an artificial compressibility term $\frac{\partial p'}{\partial t}$ which may be replaced by $\frac{1}{\beta^2} \frac{\partial p}{\partial t}$ using a numerical speed of sound β . By further introducing a dual time stepping the artificial compressibility method has been successfully applied in unsteady inviscid free surface flow problems, see [19], [20]. If an upwind-differencing scheme as for computing compressible flows is used, a slower convergence is to be expected for finer grids, see Merkle & Athavale [11] and Rogers & Kwak [13]. This implies that the method is not suitable to the solution of the Navier-Stokes equations.

Another traditional but more efficient approach to coupling the velocity and the pressure field is the so-called pressure correction method, see Caretto et al. [1] and Patankar & Spalding [12]. In this paper the well known SIMPLE-algorithm is modified to solve the three-dimensional Navier-Stokes equations on moving grid configurations. In order to avoid artificial mass sources, a space conservation law is employed to ensure a fully conservative computational procedure. The RNG k - ϵ model is used for the turbulence modelling and the fully implicit temporal differencing provides stability for any time step.

To calibrate the method, some test problems are recalculated. The computed results for a NACA0012 airfoil in pitching motion are found to be in good agreement with analytical solutions and experimental data. The results of a wave channel with a wavemaker

Revision received December 13, 2000. Open for discussion till August 31, 2002.

show that the modified SIMPLE formulation is suitable for the calculation of unsteady free surface flow problems. Finally, the proposed method is applied to the simulation of the flow interaction between a simplified arrangement of draft tube and tailwater. In order to reduce the computational time the same code runs separately on two CPUs by communicating the data via PVM libraries.

2 Governing equations

The integral form of the conservation law for mass and momentum is used to describe a flow in moving coordinates. For an arbitrarily shaped domain of volume V bounded by a closed surface A , the continuity and momentum equations are written as follows, see [6]:

$$\frac{d}{dt} \iiint_{V(t)} \rho dV + \iint_{A(t)} \rho (\vec{c} - \vec{w}) \cdot \vec{n} dA = 0, \quad (1)$$

and

$$\frac{d}{dt} \iiint_{V(t)} \rho c_i dV + \iint_{A(t)} \rho c_i (\vec{c} - \vec{w}) \cdot \vec{n} dA = \iint_{A(t)} (\tau_{ij} \vec{i}_j - \psi \vec{i}_i) \cdot \vec{n} dA. \quad (2)$$

In equations (1) and (2) ρ represents the fluid density, \vec{c} the fluid velocity and \vec{w} the net velocity, respectively. In the equation (2), the pressure variable ψ is the static pressure p plus the hydrostatic component $\rho g z$:

$$\psi = p + \rho g z. \quad (3)$$

The shear stress is defined by

$$\tau_{ij} = \mu \left(\frac{\partial c_i}{\partial x_j} + \frac{\partial c_j}{\partial x_i} \right), \quad (4)$$

where μ is the dynamic viscosity.

In the calculation, all coordinates and velocities are non-dimensionalized by reference length z_{ref} and velocity u_{ref} . The pressure variables are non-dimensionalized by ρu_{ref}^2 . Thus the non-dimensional pressure variable Ψ may be expressed as follows, see Farmer et al. [5]:

$$\Psi = P + Z / Fr^2, \quad (5)$$

where the Froude number Fr is defined by

$$Fr = \frac{u_{ref}}{\sqrt{g z_{ref}}}. \quad (6)$$

The calculations are performed on moving grid configurations. In order to avoid artificial mass sources due to the net velocity, as proposed by Demirdzic and Peric [4], a space conservation law

$$\frac{d}{dt} \iiint_{V(t)} dV - \iint_{A(t)} \vec{w} \cdot \vec{n} dA = 0 \quad (7)$$

is introduced to ensure a fully conservative computational procedure.

3 Numerical solution

The numerical procedure is based on a finite volume method for the flow variables (u , v , w , p and k , ϵ) and a finite difference method for the free surface evolution variable (h). The solutions are coupled by first computing the flow under the free surface at each pseudotime step (outer iteration), and then using the free surface velocities to calculate the movement of the free surface. After the free surface elevation is updated, its new values are used as a boundary condition for the pressure on the bulk flow for the next iteration. The entire iterative process is repeated until a prescribed convergence criterion is reached.

3.1 Bulk flow solution

A fully implicit temporal differencing makes the method stable for any time step. Applying the finite volume approach, the discretization of the convection and diffusion fluxes is carried out in a co-located variable arrangement. The momentum equation in the i -direction can be written in the following discrete form:

$$\frac{3(\Delta V \rho c_i)^{n+1} - 4(\Delta V \rho c_i)^n + (\Delta V \rho c_i)^{n-1}}{2\Delta t} + (\sum F^c)^{n+1} = [\sum F^d - \sum (\psi \vec{i}_i \cdot \vec{n} dA)]^{n+1}, \quad (8)$$

where F^c and F^d are the convective and diffusive fluxes on the surfaces of the control volumes. The convective flux F^c is calculated by applying the mass flux, which uses the net velocity, see [21].

For the computation of mass fluxes through the surfaces of a control volume, the values of the velocity components at the surface centers have to be determined. To avoid oscillations which may result from simple linear interpolation, a "Deferred Correction" scheme first proposed by Khosla and Rubin [10] is implemented, see Ferziger and Peric [6]:

$$c^{s+1} = c_L^{s+1} + \beta (c_H - c_L)^s. \quad (9)$$

In this equation c_L stands for an interpolation of a lower order scheme (e.g. "upwind") and c_H a higher order approximation. The term in the brackets with superscript "s" is calculated "explicitly" from values of a previous iteration. Multiplying the term in the brackets by the blending factor β controls the "explicit" and implicit contributions. The use of this "Deferred Correction" scheme damps oscillations and improves the diagonal dominance of the coefficient matrix. In this way, the stability of the algorithm can be enhanced while maintaining sufficient accuracy.

The coupling of the pressure and the velocity is performed via the SIMPLE algorithm given in [1], [12]. The continuity equation is

transformed into a pressure correction equation which has the same general form as the discretized momentum equations. The use of the co-located variable arrangement on non-orthogonal grids demands the SIMPLE algorithm be slightly modified. Here, a pressure-velocity coupling method for complex geometries used by Ferziger and Peric [6] is implemented, where an additional pressure gradient term is subtracted from the velocity value at the surface of control volume. On the other hand, the space conservation law (Eq. 4) is enforced in the pressure correction equation for moving grids to ensure the conservation of mass, see [21]. The transport equations of the turbulence modelling for k and ε are discretized similar to the momentum equations:

$$\frac{d}{dt} \iiint_{V(t)} \rho k dV + \iint_{A(t)} [\rho k (\vec{c} - \vec{w}) - \Gamma_k \text{grad} k] \cdot \vec{n} dA = \iiint_{V(t)} (P_k - \rho \varepsilon) dV, \quad (10)$$

$$\frac{d}{dt} \iiint_{V(t)} \rho \varepsilon dV + \iint_{A(t)} [\rho \varepsilon (\vec{c} - \vec{w}) - \Gamma_\varepsilon \text{grad} \varepsilon] \cdot \vec{n} dA = \iiint_{V(t)} \frac{\varepsilon}{k} (c_{\varepsilon 1} P_k - c_{\varepsilon 2} \rho \varepsilon) dV, \quad (11)$$

$$\mu_t = \rho c_\mu \frac{k^2}{\varepsilon}, \quad (12)$$

where Γ_k , Γ_ε and ρ_k are as follows

$$\Gamma_k = \mu_l + \frac{\mu_t}{\sigma_k}, \quad \Gamma_\varepsilon = \mu_l + \frac{\mu_t}{\sigma_\varepsilon}, \quad (13)$$

$$P_k = \tau_{i,j} \frac{\partial c_i}{\partial x_j}. \quad (14)$$

For the computations the RNG variant of the k - ε turbulence model is used. The empirical constants of this non-linear model proposed by Yakhot et al. [18] are given in Table 1, where the coefficient η depending on the stresses is defined as

$$\eta = \frac{Dk}{\varepsilon} \quad (15)$$

with

$$D = (2D_{ij} D_{ij})^{1/2}, \quad D_{ij} = \frac{1}{2} \left(\frac{\partial c_i}{\partial x_j} + \frac{\partial c_j}{\partial x_i} \right). \quad (16)$$

Table 1 Empirical constants of the non-linear RNG k - ε turbulence model

c_μ	σ_k	σ_ε	$c_{\varepsilon 1}$	$c_{\varepsilon 2}$
0.085	0.7179	0.7179	$1.42 - \frac{\eta(1-\eta/\eta_0)}{1+\beta\eta^3}$	1.68

The coefficient η_0 is set equal to 4.38, so that for $\beta = 0.12$ the von Karman constant is equal to 0.4.

In order to reduce the computational time, the PVM (Parallel Virtual Machine) libraries are implemented. The calculation of the draft tube and tailwater flow can be carried out in parallel on two computers, each using the same code and communicating the data of the inner boundary between the draft tube and tailwater via PVM interface.

3.2 Free surface solution

Both a dynamic and kinematic boundary condition are imposed at the free surface. The dynamic condition states that the static pressure acting on the free surface is constant:

$$P = P_{air} = \text{constant}. \quad (17)$$

Since the free surface location is defined by

$$z = h(x, y, t), \quad \text{i.e. } Z = H(X, Y, T), \quad (18)$$

the dynamic condition on the free surface can be expressed in dimensionless form as follows, see equations (5) and (17):

$$\Psi = P_{air} + H / Fr^2. \quad (19)$$

The kinematic condition is derived from equation (18):

$$w = \frac{\partial h}{\partial t} + u \frac{\partial h}{\partial x} + v \frac{\partial h}{\partial y}. \quad (20)$$

The kinematic condition states that the free surface is a material surface, i.e. once a fluid particle is on the free surface, it remains on the surface forever. This kinematic equation is used for calculating the free surface development.

The calculations are performed in moving grid systems. In a moving grid system, this formulation can be expressed as

$$h_\tau = w - (u - x_\tau) h_x - (v - y_\tau) h_y, \quad (21)$$

where x_τ and y_τ are the components of net velocity. So as the solution for the bulk flow under the free surface, a three time level scheme is applied to the calculation for the free surface:

$$\frac{3h^{n+1} - 4h^n + h^{n-1}}{2\Delta\tau} = [w - (u - x_\tau) h_x - (v - y_\tau) h_y]^{n+1}. \quad (22)$$

Throughout the interior of the (x, y) plane, the derivatives h_x and h_y are computed using the second-order central difference stencil in computational coordinates ξ and η . To prevent oscillatory solutions dissipative terms are introduced in the right hand side of equation (21):

$$h_\tau = w - (u - x_\tau)h_x - (v - y_\tau)h_y + \frac{|u - x_\tau| \Delta x}{2} h_{xx} + \frac{|v - y_\tau| \Delta y}{2} h_{yy}. \quad (23)$$

On the boundary of the (x,y) plane, the free surface location is extrapolated from the interior area.

4 Boundary conditions

The solution of the Navier-Stokes equations necessitates appropriate boundary conditions to make the resulting system of algebraic equations solvable. In this paper velocity profiles are assumed at the inflow and the static pressure is specified at the outflow, while other components are extrapolated normally by assuming zero gradient. On the wall, the boundary conditions of impermeability and no-slip are defined for the velocity, and the normal gradient of pressure is assumed to be zero.

For the turbulence modelling, k is usually assumed to be small at the inlet, say $6 \times 10^{-4} \times u_{in}^2$ in this study. The value of ε at the inlet is evaluated from

$$\varepsilon = \frac{k^{3/2}}{L}, \quad (24)$$

where L is the length scale. At the exit, the values of k and ε are evaluated by extrapolating from the interior nodal values. The law of the wall is applied in near-wall regions. In the viscous sub-layer, the logarithmic profile no longer holds. As in TASCflow [16] a three layer form is used:

$$\begin{cases} u^+ = n^+ & \text{for } n^+ \leq 5, \\ u^+ = d_1(n^+)^3 + d_2(n^+)^2 + d_3n^+ + d_4 & \text{for } 5 < n^+ \leq 30, \\ u^+ = \frac{1}{\kappa} \ln(n^+) + C & \text{for } n^+ > 30, \end{cases} \quad (25)$$

where $n^+ = nu_\tau/\nu$, $u^+ = u/u_\tau$. u_τ is the friction velocity constructed from the wall stress in the standard manner: $u_\tau = \sqrt{\tau_{wall}/\rho}$. u_i is the velocity component tangential to the wall and n the distance from the wall, ν is the kinematic viscosity. These functions are used to establish boundary conditions for k and ε at the first grid points away from the wall as well as for the wall shear stress τ_{wall} which is used for integrating the momentum equations. The empirical constants $d_{1,2,3,4}$ are determined such that three equations yield a continuous development of $u^+(n^+)$ in the range $0 < n^+ < 500$, see [16]. They are listed in Table 2.

Table 2: Empirical constants of the wall functions

κ	C	d_1	d_2	d_3	d_4
0.41	5.2	6.43×10^{-4}	-5.21×10^{-2}	1.47	-1.14

5 Validation of the numerical procedure / developed CFD-codes

Both incompressible viscous unsteady flow problems with and without free surfaces are considered in order to assess the accuracy and efficiency of the developed numerical procedures.

5.1 Flow over a NACA0012 airfoil

The flow over a NACA0012 airfoil with a semichord $b = 0.5$ m is considered. A uniform free stream with a velocity $u_\infty = 1$ m/s is impinging on the airfoil which is pitching about an axis located at 37 percent chord with a reduced frequency $k_c = \omega b / u_\infty = 0.4$, where ω is the angular frequency of the forced motion of the airfoil. The amplitude of the motion is chosen to be 6.74 degrees. The analytical solutions and experimental results have been reported by Halfman [7]. An O-mesh with $81 \times 20 \times 11$ points is used in the calculation. The inner part of the O-mesh shown in Figure 1 is pitching together with the airfoil. A plot of the lift coefficient versus the angle of attack computed during the third pitching cycle using the developed procedures for the Navier-Stokes solution in this study is presented in Figure 2. The Euler solution is obtained using a modified artificial compressibility method proposed in [20], [21].

5.2 Wave channel

An unsteady free surface problem in a wave channel is performed with $179 \times 11 \times 11$ moving grids. This wave problem has been experimentally investigated by Chapalain [2] in a 35.54 m long and 40 cm deep tank with a piston-type wavemaker which sinusoidally oscillates with 7.8 cm amplitude and 2.5 s period, see Figure 3. Figure 4 and Figure 5 show the comparison between the experimental and the computed wave profiles at four different x locations as a function of time.

6 Simulation of the interaction between the draft tube and tailwater flow

According to the theoretical and experimental investigations of

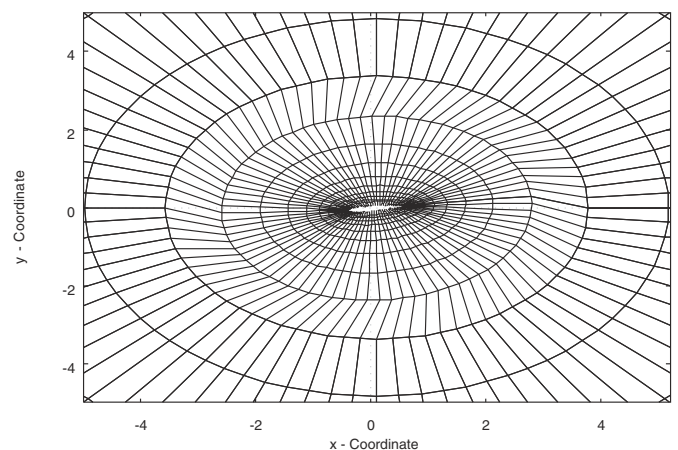


Fig. 1 Mesh of the NACA0012 Airfoil in Pitching Motion.

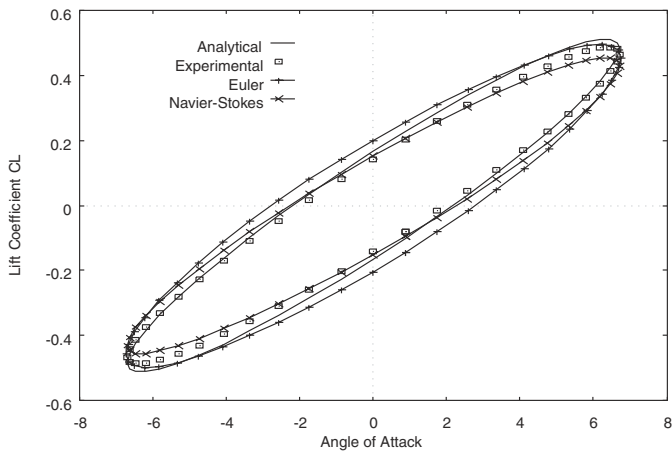


Fig. 2 Lift coefficients of the NACA0012 Airfoil in Pitching Motion.

Schneider et al. [14], [15] and Toyokura et al. [17] there exists a significant interaction of the draft tube and tailwater flow. To verify the developed code, a test case of Toyokura et al. [17] is considered.

The experimental model of the open channel is shown in Figure 6. The water was supplied by a pump. The water through the honeycomb located at the draft tube inlet flows out into the open channel. A square duct, which has a side length “a”, is used as the draft tube, and its dimension is changed into 2 types ($a=105, 108$ mm). The bottom plate of the draft tube is accorded with the bottom height of the open channel. The side walls of the open channel may be moved to change the width “b”. The water level \bar{H}_s in the open channel may be adjusted by a movable weir plate set in the downstream. The measurement device which makes use of the water conductivity was used for measuring the height of the free surface.

As a test example, a draft tube and tailwater flow with $u_{in}=1$ m/s is calculated for the geometry of $b/a=2.0$, $a=188$ mm and $\bar{H}_s=2.0$. The velocity distributions on the vertical plane A-A in the passage center and the horizontal plane C-C at the draft tube middle height are shown in Figures 7-9. In the figures, the water flowing out from the draft tube diffuses gradually as a jet flow, and the large reverse flow region can be observed at the upside of the jet flow. On the other hand, the jet flow reaches rapidly the side walls because the open channel width is not wide.

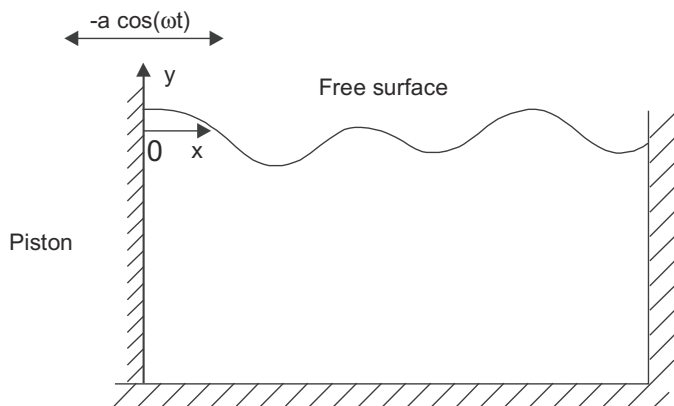


Fig. 3 Schema of Chapalain's test case [2].

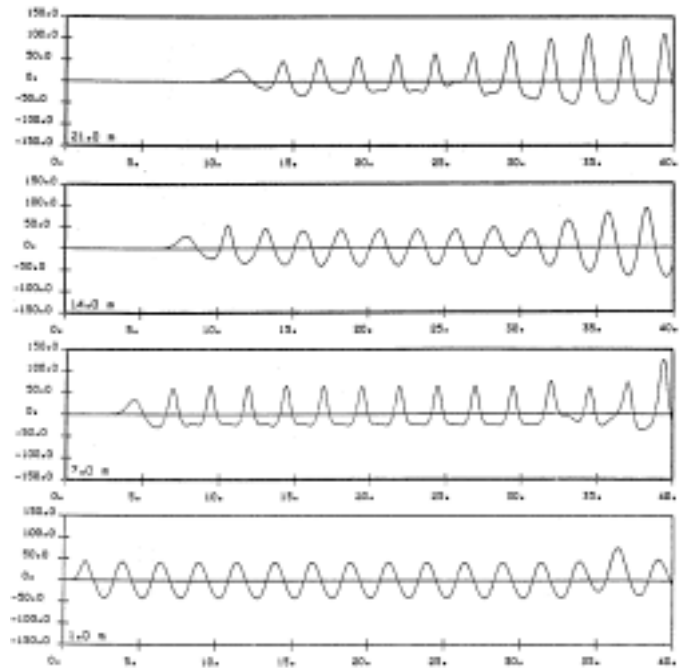


Fig. 4 Measured wave profiles at 4 x-positions, from Chapalain [2].

The water level measured by Toyokura et al. [17] is given by the marks “ \diamond ” in Figure 8. It shows that the computed water level coincides with the measured data fairly well. Owing to the diffusion of the jet flow, the water level in the open channel increases gradually in accordance with the decrease of velocity head. This means, the expanding jet downstream the draft tube exit can be considered as an extended diffuser. The continued deceleration of the flow results in a depression of the water level at the draft tube exit, thus increasing the net head.

To study the influences of the tailwater parameters, turbine dis-

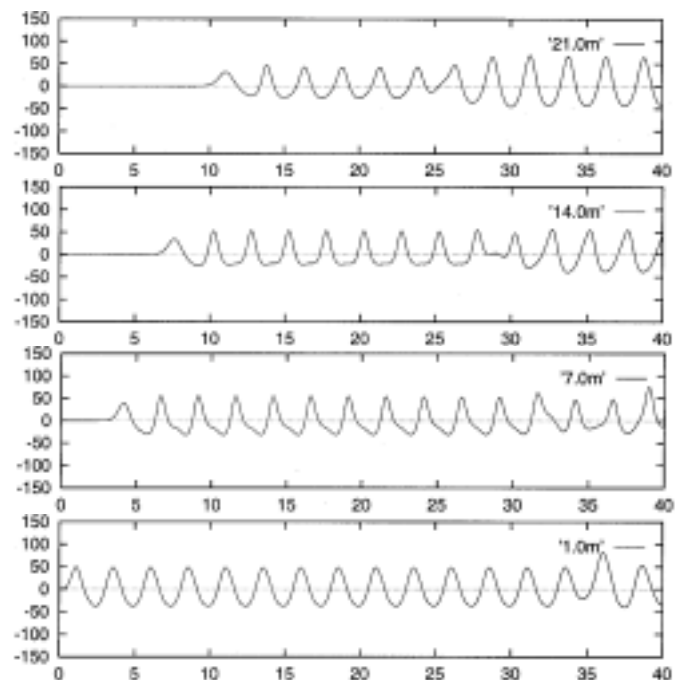


Fig. 5 Computed wave profiles at 4 x-positions.

flow conditions and the results are given in Table 4. It shows that the water level rise Δh_{tw} indicating the head recovery in the tailwater increases, if the inlet flow velocity u_{in} becomes bigger. This means that the head recovery becomes more important at operating points $Q \geq Q_{opr}$.

Table 4: Water level rises for different inlet velocities

u_{in} (m/s)	Δh_{tw} (mm) only tailwater	Δh_{tw} (mm) with draft tube	Deviation (%)
0.9	10.88	11.13	2.2
1.0	13.42	13.61	1.4
1.1	16.15	16.26	0.7

In each case the tailwater flow calculations are carried out with and without considering the draft tube flow. Table 4 also shows the deviation of the decoupled computations from the coupled ones. This deviation increases due to the non-uniform velocity distribution at the interface between the draft tube and tailwater. In a real water power plant a larger deviation may be expected. This deviation indicates that a decoupled solution is not suitable to the optimization of the tailwater flow in the water power plants.

6.3 Influence of the draft tube swirl

In accordance with the results presented by Schneider [14], the swirl and the radial velocity components at the draft tube exit tend to expand the emerging jet. In order to check the effect of the draft tube swirl, in other words the cross velocity, on the head recovery, a calculation is carried out for the geometry used above. Here a distribution of the velocity components normal to the main flow at the draft tube inlet with $v_{in,max} = 0.1$ m/s is assumed instead of the swirl flow components, see Figure 10. Table 5 shows the influence of the normal velocity components on the water level rise Δh_{tw} .

Table 5: Influence of the normal velocity components

u_{in} (m/s)	$v_{in,max}$ (m/s)	Δh_{tw} (mm)
1.0	0.0	13.61
1.0	0.1	13.81

The balance of the water level rise Δh_{tw} in the tailwater and the waste energy loss Δh_{loss} at the inlet of draft tube, or in other words, at the runner exit, can be performed as

$$\Delta h_{loss} = \frac{\iint_{A_{in}} \frac{1}{2g} (u^2 + v^2) \rho u dA - \iint_{A_{in}} \frac{1}{2g} u^2 \rho u dA}{\iint_{A_{in}} \rho u dA} = 0.17 \text{ mm},$$

and

$$\Delta(\Delta h_{tw}) = 13.81 - 13.61 = 0.20 \text{ mm} > \Delta h_{loss}$$

This analysis reveals a positive effect of the swirl on the head

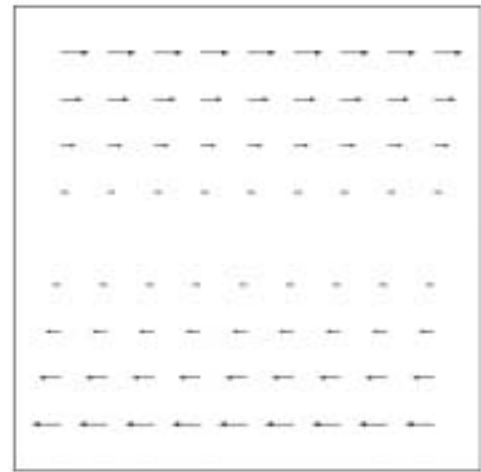


Fig. 10 Assumed distribution of the velocity components normal to the main flow at the draft tube inlet.

recovery. This result agrees qualitatively with the findings of Schneider [14], [15]. A more correct and reliable prediction of the energy losses in the draft tube and the water level rise in the tailwater is still a problem since the turbulence modelling for swirling flows is not accurate enough.

7 Conclusion

An approach using pressure correction based on the finite volume method has been proposed for the solution of incompressible free surface flow problems. The $k-\epsilon$ model is applied for the turbulence modelling. The flow field is solved by coupling the free surface kinematic and dynamic conditions.

The proposed method has been applied to the prediction of the interaction between the draft tube and tailwater flow. Numerical simulations show that the jet downstream the draft tube acts as an extended diffuser with a free surface, thus decreasing the water level at the turbine exit. The energy in the tailwater flow is partially recoverable. Larger values of head recovery are expected by smaller submergence of turbine. The draft tube swirl to some extent affects the head recovery in the tailwater positively.

The presented method appears to be suitable for the simulation of the interaction between the draft tube and tailwater flow. The method bases on the time marching technique, therefore it also can be used directly to simulate unsteady flow effects, see [21]. A better prediction of the flow field could be obtained by improving the turbulence model as well as the treatment of the interaction between the turbulent flow and the free surface in the tailwater.

Acknowledgement

The scholarship from German Academic Exchange Service (Deutscher Akademischer Austauschdienst) awarded to the first author during this study at the University of Technology Munich is gratefully acknowledged. The valuable suggestions and modifications of Prof. Can F. Delale from the Istanbul University and

Dr. Wen Chen of the Rensselaer Polytechnic Institute to the English-text for the preparation of this paper is also appreciated.

Notations

a	width and height of draft tube
A	surface of control volume
AR_{tw}	tailwater area ratio
b	width of tailwater; semichord of NACA0012 airfoil
c	velocity
$c_\varepsilon, c_{\varepsilon 1}, c_{\varepsilon 2}$	constants of turbulence model
c_H	interpolation of a higher order
c_L	interpolation of a lower order
C	constant of the law of the wall
d_1, d_2, d_3, d_4	constants of the wall functions
F^c	convective flux
F^d	diffusive flux
Fr	Froude number
g	acceleration of gravity
h	water level height
h_x, h_y	derivatives of free surface
h_τ	net velocity on free surface
H	dimensionless water level height
\bar{H}_s	water level at draft tube exit
\bar{i}	unit vector of coordinates
k	turbulence kinetic energy
k_c	reduced frequency
L	length scale for turbulence modelling
n	vertical distance from the wall
\bar{n}	unit vector of cell face
n^+	nu_τ / ν
p	static pressure
P	dimensionless static pressure
P_{air}	dimensionless atmospheric pressure
P_k	turbulence production
Q	volume discharge
t	time
T	dimensionless time
u, v, w	velocity components
u_t	velocity component tangential to the wall
u_τ	shear velocity
u^+	u_t / u_τ
u_∞	velocity in far field
u_{ref}	reference velocity
V	volume
w	net velocity
x, y, z	coordinates
x_τ, y_τ	net velocity components
X, Y, Z	dimensionless coordinates
z_{ref}	reference length
Δh	water level rise
β	artificial speed of sound; blending factor; constant for turbulence modelling
η	coefficient depending on stress
η_0	coefficient for turbulence modelling
ε	turbulence dissipation rate

τ	shear stress; time
ν	kinematic viscosity
μ	dynamic viscosity
ρ	density
$\sigma_k, \sigma_\varepsilon$	constants of turbulence model
κ	von Karmen constant
ω	angular frequency
ψ	pressure variable
Ψ	dimensionless pressure variable
$\Gamma_k, \Gamma_\varepsilon$	diffusion coefficients of turbulence model

Subscripts

i, j	indices indicating directions: $i, j = 1, 2, 3$
in	inflow
l	laminar component
t	turbulent component
tw	tailwater

Superscripts

n	index of time level
s	index of pseudotime level, i.e. outer iteration

References

- CARETTO, L. S., GOSMAN, A. D., PATANKAR, S. V. and SPALDING, D. B.: Two Calculation Procedures for Steady, Three-Dimensional Flows with Recirculation, Proceedings of the 3rd Intern. Conf. on Numerical Methods in Fluid Mechanics, Vol. 2, Paris, July 3-7, 1972, in Lecture Notes in Physics 19, Springer-Verlag.
- CHAPALAIN, G.: Etude hydrodynamique et sédimentaire des environnements littoraux dominés par la houle, Thèse de Doctorat de l'Université Joseph Fourier, Grenoble, 1988, (in French).
- CHORIN, A. J.: A Numerical Method for Solving Incompressible Viscous Flow Problems, Journal of Computational Physics, Vol. 2, pp. 12-26, 1967.
- DEMIRDZIC, I., PERIC, M.: Finite Volume Method For Prediction of Fluid Flow in Arbitrarily Shaped Domains with Moving Boundaries, International Journal for Numerical Methods in Fluids, Vol. 10, pp. 771-790, 1990.
- FARMER, J., MARTINELLI, L. and JAMESON, A.: Fast Multigrid Method for Solving Incompressible Hydrodynamic Problems with Free Surfaces, AIAA Journal, Vol. 32, No. 6, June 1994.
- FERZIGER, J. H., PERIC, M.: Computational Methods for Fluid Dynamics, Springer-Verlag, Berlin Heidelberg, 1996.
- HALFMAN, R. L.: Experimental Aerodynamic Derivatives of a Sinusoidally Oscillating Airfoil in Two-Dimensional Flow, NACA Report 1108, 1952.
- HIRT, C. W., NICHOLS, B. D.: Volume of Fluid (VOF) Method for the Dynamics of Free Boundaries, Journal of Computational Physics, Vol. 39, pp. 201-225, 1981.
- KITA, E., KUBOTA, K., KIMOTO, Y.: Tailwater Level and

- Net Head in Low Head Power Plant, Proceedings of the 3rd Japan-China Joint Conference on Fluid Machinery, Vol. 1, Osaka, 1990.
10. KHOSLA, P. K. and RUBIN, S. G.: A Diagonally Dominant Second-Order Accurate Implicit Scheme, *Computers & Fluids*, 2, pp. 207, 1974.
 11. MERKLE, C. L., ATHAVALE, M.: Time-Accurate Unsteady Incompressible Flow Algorithms Based On Artificial Compressibility, AIAA Paper 87-1137.
 12. PATANKAR, S. V. and SPALDING, D. B.: A Calculation Procedure for Heat, Mass and Momentum Transfer in Three-Dimensional Parabolic Flows, *International Journal of Heat Mass Transfer*, 15, pp. 1787-1806, 1972.
 13. ROGERS, S. E., KWAK, D.: Steady and Unsteady Solutions of the Incompressible Navier-Stokes Equations, *AIAA Journal*, Vol. 29, Nr. 4, April 1991.
 14. SCHNEIDER, Ch.: Untersuchung der Wechselwirkung schnelllaufender Wasserturbinen mit dem Unterwasser, Ph. D. thesis, Technische Universitaet Muenchen, 1997, (in German).
 15. SCHNEIDER, Ch., MOCHKAAI, Y., KNAPP, W., SCHILLING, R.: Head Recovery in the Tailwater of Low Head Hydro Power Stations, *Energy and Water: Sustainable Development*, 27th IAHR Congress, San Francisco, 10-15 August 1997.
 16. TASCflow (ASC): Theory Documentation, Version 2.4, Waterloo Ontario, Canada, 1995.
 17. TOYOKURA, T., KITAHORA, T., YAMAZAWA, H., KUBOTA, T., SUZUKI, R.: Flow in Open Channel near Draft Tube Outlet of Low Head Turbine, IAHR and AIRH Symposium 1990, Belgrade, Yugoslavia.
 18. YAKHOT, V. and ORSZAG, S. A., THANGAM, S., GATSKI, T. B. and SPEZIALE, C. G.: Development of Turbulence Models for Shear Flows by a Double Expansion Technique, *Phys. Fluid A4* (7), July 1992.
 19. YUAN, W., RIEDEL, N., SCHILLING, R.: Time Accurate Simulation of Free Surface Flow Problem, *Energy and Water: Sustainable Development*, 27th IAHR Congress, San Francisco, 10-15 August 1997.
 20. YUAN, W., SCHUSTER, M., YANG, C., SCHILLING, R.: Three-Dimensional Time Accurate Simulation for Unsteady Incompressible Flow, *Third International Conference on Hydroscience and Engineering*, Cottbus/Berlin, 31. Aug. - 3. Sept. 1998.
 21. YUAN, W.: Simulation der Saugrohr-Unterwasser-Wechselwirkung, Ph. D. thesis, Technische Universitaet Muenchen, 1999, (in German).